

# Comparison of Fluorine-18-Fluorodeoxyglucose and Carbon-11-Methionine in Head and Neck Cancer

Paula Lindholm, Sirkku Leskinen-Kallio, Heikki Minn, Jörgen Bergman, Merja Haaparanta, Pertti Lehtikoinen, Kjell Någren, Ulla Ruotsalainen, Mika Teräs and Heikki Joensuu

Department of Oncology and Radiotherapy, Turku University Central Hospital, Turku University Cyclotron/PET Center, Turku University Central Hospital and Turku University Cyclotron/PET Center, Radiopharmaceutical Chemistry Laboratory, Turku, Finland

The positron emission tomography (PET) tracer 2-<sup>18</sup>F-fluoro-2-deoxy-D-glucose (FDG) is the most widely used tracer in oncology. PET tracer. Another radiotracer, L-methyl-<sup>11</sup>C-methionine (<sup>11</sup>C-methionine), also has been used successfully for PET imaging of brain and lung tumors, non-Hodgkin's lymphoma, breast cancer and head and neck cancer. This study compared FDG and <sup>11</sup>C-methionine as tumor-detecting agents in head and neck cancer. Prior to cancer therapy, fourteen patients underwent a PET study with FDG and one with <sup>11</sup>C-methionine. Nineteen of 21 malignant lesions that could be evaluated were visible with both tracers. Tracer uptake was measured as standardized uptake values (SUV) and K<sub>i</sub> values according to Patlak et al. The mean SUV in FDG studies was 7.7 ± 4.2 and in <sup>11</sup>C-methionine studies 7.7 ± 2.5, whereas the K<sub>i</sub> values in <sup>11</sup>C-methionine studies (mean, 0.128 ± 0.068 min<sup>-1</sup>) were always higher than in FDG studies (mean, 0.036 ± 0.023 min<sup>-1</sup>). A good correlation was found between the SUVs ( $r = 0.79$ ,  $p < 0.0001$ ) and the K<sub>i</sub> values ( $r = 0.82$ ,  $p < 0.001$ ) between the two tracers. Both FDG and <sup>11</sup>C-methionine are effective in PET imaging of head and neck cancer, and the uptake rates of the tracers seem to be closely related.

J Nucl Med 1993; 34:1711-1716

The most widely used radiopharmaceutical for studies on tumor metabolism with positron emission tomography (PET) is 2-<sup>18</sup>F-fluoro-2-deoxy-D-glucose (FDG), and its role as a tumor-seeking agent has been established in many different types of cancer (1). Because of its low rate of dephosphorylation, FDG is transported, phosphorylated and metabolically trapped into tumor cells as fluorodeoxyglucose-6-phosphate (2).

FDG uptake has been reported to correlate with the histological grade of gliomas (3); it may also predict the survival rate of patients with high-grade brain tumor (4).

Similarly, FDG uptake appears to correlate with histological grading of non-Hodgkin's lymphomas (5), musculoskeletal tumors (6-7) and liver tumors (8), but not with lung (1) or head and neck tumors (9-10).

Another useful tracer for oncologic PET studies is L-methyl-<sup>11</sup>C-methionine (<sup>11</sup>C-methionine). Methionine is an essential amino acid that is needed for polyamine and protein synthesis, and transsulphuration and transmethylation reactions. Tumor cells have altered overall transmethylation and methionine metabolism (11), and the increased <sup>11</sup>C-methionine utilization of cancerous tissue can be measured by PET (12-13).

Carbon-11-methionine has been successfully used for metabolic imaging of brain and lung tumors (12-13), non-Hodgkin's lymphoma (5), breast cancer (14) and head and neck cancer (15). The uptake of <sup>11</sup>C-methionine appears to correlate with the histological grade of brain (16) and lung tumors (17). However, <sup>11</sup>C-methionine uptake had no significant association with the histological grading of non-Hodgkin's lymphomas (5) or head and neck cancer (15).

The present study compared FDG and <sup>11</sup>C-methionine as tumor-detecting tracers in head and neck cancer and compared tracer uptake with histological grade of the tumors.

## MATERIALS AND METHODS

### Patients

Fourteen patients with head and neck cancer were studied using both FDG and <sup>11</sup>C-methionine before cancer therapy was initiated. Each patient signed informed consent for the study, which was approved by the Ethical Committee of Turku University Central Hospital.

Eleven of the 14 patients had squamous cell carcinoma, one had acinar cell carcinoma, one adenocarcinoma of the nasal cavity, and one malignant schwannoma in the neck (Table 1). Four patients had recurrent cancer. One of the four (Patient 7), who previously had been treated for tonsillar cancer, had only bilateral cervical lymph node metastases at the time of study. Six patients with primary cancer also had regional lymph node metastases. Patient 8 had large squamous-cell cancer of the skin and metastases in the lymph nodes of the neck located so close to each other

Received Jan. 6, 1993; revision accepted June 17, 1993.  
For correspondence and reprints contact: Paula Lindholm, MD, Department of Oncology and Radiotherapy, Turku University Central Hospital, SF-20520 Turku, Finland.

**TABLE 1**  
Patient Characteristics

Patient	Age/sex	BMI*	Site of tumor	Size (cm)	Histology <sup>†</sup>	Stage <sup>‡</sup>	Grade <sup>§</sup>
1	67/M	22.7	Nasal cavity	7 × 6	AC	T4N0M0	II
2	38/M	20.9	Tongue	7 × 4	SCC	T3N1M0	II
			Neck metastasis, right	2 × 3			
3	49/F	21.5	Hypopharynx	12 × 2	SCC	T4N0M0	II
4	79/M	23.7	Nasopharynx	6 × 4	SCC	T4N2M0	III
			Neck metastasis, right	1.5 × 1			
			Neck metastasis, left	1.5 × 1			
5	62/F	35.1	Neck	8 × 7	MS	T2N0M0	III
6	80/M	25.4	Skin of face	2 × 2	ACC	rT1N0M0	I
7	68/M	17.0	Neck metastasis, right	1.5 × 1	SCC	rT3N2M0	III
			Neck metastasis, left	3.5 × 2.5			
8	83/M	24.7	Skin of face	6 × 7	SCC	rT2N1M0	I
			Neck metastasis, right	2 × 2			
9	67/M	28.4	Parotid gland	6 × 7	SCC	T3N2M0	I
			Neck metastases, right	1.5 × 1.5			
10	63/M	28.4	Upper gum	1.5 × 1	SCC	T1N1M0	I
			Neck metastasis, left	2 × 2			
11	58/F	28.9	Floor of mouth	2 × 1	SCC	T1N0M0	II
12	71/F	26.7	Nasopharynx	5 × 4	SCC	T3N2M0	III
			Neck metastases <sup>¶</sup>	1.5–3 × 3–4			
13	50/M	22.3	Hypopharynx	8 × 1.5	SCC	T4N1M0	I
			Neck metastasis, left	2 × 2			
14	80/M	25.3	Neck metastasis, right	8 × 6	SCC	rT1N3M0	II

\*BMI, body mass index (18).

<sup>†</sup>Histology: AC = adenocarcinoma; SCC = squamous-cell carcinoma; MS = malignant schwannoma; and ACC = acinar cell carcinoma.

<sup>‡</sup>Stage by UICC (19); r = recurrent.

<sup>§</sup>Grades I, II and III; well, moderately and poorly differentiated, respectively.

<sup>¶</sup>Several bilateral neck metastases.

that it was impossible to distinguish the margins between the primary tumor and its metastasis. All primary and metastatic tumors were histologically or cytologically verified by a biopsy. Altogether there were 21 malignant lesions in 14 patients.

None of the patients had diabetes. Patient 9 had slightly elevated blood glucose level (7 mmol/liter, reference range, from 3.3 to 6.4 mmol/liter) during the FDG study; all others were euglycemic. The body mass index (BMI) (18) calculated as:

$$\text{BMI} = \frac{\text{weight (kg)}}{(\text{height})^2 (\text{m}^2)}$$

varied between 17.0 and 35.1 (mean, 25.1). Clinical staging was performed according to the UICC TNM classification of malignant tumors (19), and it included careful physical examination, endoscopy, ultrasonography, computed tomography (CT) and magnetic resonance imaging (MRI) when feasible.

### PET Imaging and Methods

The PET scanner was an ECAT type 931/08-12 (Siemens/CTI, Knoxville, TN), which produces 15 contiguous slices with a slice thickness of 6.7 mm and an in-plane resolution of 6.1 mm FWHM in the center of the field of view. Both the tracers were synthesized at the Radiopharmaceutical Chemistry Laboratory of Turku University Cyclotron/PET Center. The FDG synthesis was a modification of the method reported by Hamacher et al. (20). The radiochemical purity of FDG was 99.1% ± 0.3% (21). Carbon-11-methionine was synthesized as described by Långström et al. (22)

with slight modifications. The radiochemical purity of <sup>11</sup>C-methionine was 97.1% ± 2.6%.

Prior to cancer treatment, every patient underwent a PET study with FDG and another with <sup>11</sup>C-methionine in random order. PET-FDG studies were performed in the fasting state. Patients had a light, protein-poor breakfast 3–5 hr before PET scanning with <sup>11</sup>C-methionine. A transmission scanning for attenuation correction was performed with a removable germanium-68 ring source. After transmission, a bolus injection of FDG (240–330 MBq) or <sup>11</sup>C-methionine (240–310 MBq) was given in a peripheral vein of the arm and dynamic emission scanning started immediately. The dynamic scanning with FDG was performed for 60 min (4 × 30 sec scans, 3 × 60 sec, 5 × 180 sec, 8 × 300 sec) and with <sup>11</sup>C-methionine for 40 min (4 × 30 sec, 3 × 60 sec, 5 × 180 sec, 4 × 300 sec). The second PET study was conducted within 1 to 15 days (median, 5.5 days) as calculated from the first PET study except in Patient 12 (for practical reasons, 23 days). Patient 1, who had both PET studies the same day, entered first into a <sup>11</sup>C-methionine study and four hours later into a FDG study.

Frequent blood samples measuring input function of the tracer were drawn from a peripheral vein of the arm opposite to the injection site; a heating pad was used to warm up the arm. In the <sup>11</sup>C-methionine studies the low molecular weight fraction of plasma taken at 20, 40 and 60 min after injection was separated by fast-gel filtration using Sephadex PD-10 columns (Pharmacia Fine Chemicals, Uppsala, Sweden), and the radioactivity concentration of this fraction was used to correct input function (5,15). In

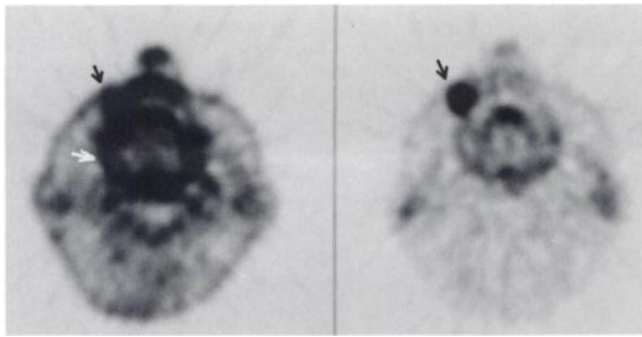


**FIGURE 1.** PET images of Patient 6. The recurrent acinar cell cancer (black arrow) in the upper lip is better visible in the  $^{11}\text{C}$ -methionine study (right) than in the FDG study (left) in which high FDG accumulation is seen in nasal and gingival mucosa (white arrow).

the FDG studies, plasma glucose concentrations were measured immediately before FDG injection. Regions of interest (ROI) were drawn on tumorous tissue representing the area of highest accumulation. The relative standard deviation of the measured average radioactivity concentration in a ROI was less than 9% in the last frame.

Tracer accumulation was measured using the standardized uptake value (SUV):

$$\text{SUV} = \frac{\text{Radioactivity concentration in ROI [Bq cm}^{-3}\text{]}}{\text{Injected dose [Bq]/Patient's weight [g]}}$$

The ROI with the maximum average radioactivity concentration in the tumor at 55–60 min (FDG) or 35–40 min ( $^{11}\text{C}$ -methionine) postinjection, corrected for calibration and decay, was chosen for the SUV analysis.

Uptake rates of the tracers were calculated as influx constants ( $K_i$  values) using the graphical approach described by Patlak et al. (23). The last 11 (FDG) or 7 ( $^{11}\text{C}$ -methionine) data points, representing the time between 11 and 60 min (FDG) or 11–40 min ( $^{11}\text{C}$ -methionine) after tracer injection, were used to produce the influx curve. In Patient 1, the  $K_i$  value of the  $^{11}\text{C}$ -methionine study could not be calculated because the radioactivity concentration was not measured in the low molecular weight fraction of plasma. In Patient 12, the influx constant of the  $^{11}\text{C}$ -methionine study could not be obtained because of technical problems.

The SUVs and the  $K_i$  values of each tracer were compared by linear regression. Wilcoxon signed-rank sum test for paired data

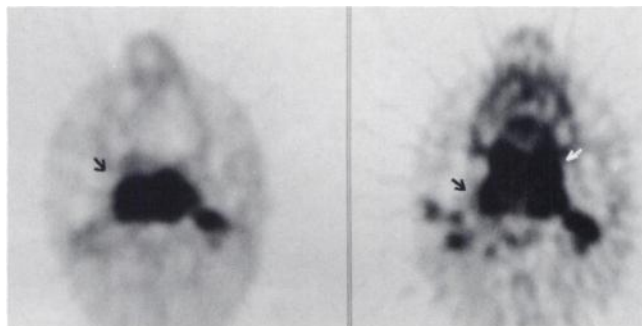


**FIGURE 2.** The nasopharyngeal cancer (black arrow) of Patient 4 is more clearly visualized in the FDG study (left) than in the  $^{11}\text{C}$ -methionine study (right). The strong accumulation of  $^{11}\text{C}$ -methionine in the hard palate (white arrow) impairs tumor delineation.

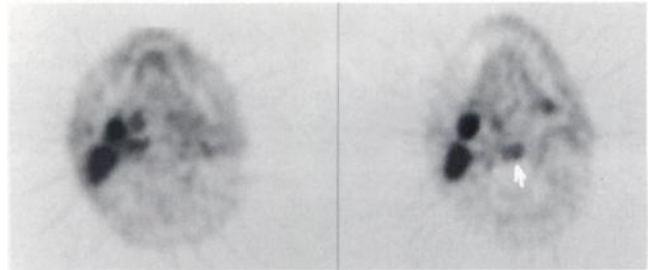


**FIGURE 3.** PET images of a large lymph node metastasis on the right side of the neck (Patient 14) studied with FDG (left) and  $^{11}\text{C}$ -methionine (right). A cervical vertebra (white arrow) is also visible in the  $^{11}\text{C}$ -methionine study.

was used to compare the uptake rates of FDG and  $^{11}\text{C}$ -methionine in the same tumor.

## RESULTS

All primary tumors and all known neck metastases were visualized with both tracers with one exception. Patient 7 had bilateral neck metastases, but the metastasis on the right side of the neck was visible only with  $^{11}\text{C}$ -methionine and the metastasis on the left only with FDG. The primary tumor of Patient 11 was not visible in CT images, but it was visualized in both PET studies. The malignant schwannoma of Patient 5 and the acinar cell cancer of Patient 6 (Fig. 1) visualized clearer in  $^{11}\text{C}$ -methionine studies, but the nasopharyngeal cancer of Patient 4 (Fig. 2) and cancer of the upper gum (Patient 10) visualized clearer in FDG studies. Usually there were no significant differences in tumor imaging (Figs. 3 and 4).

The SUVs of the tumors in FDG studies varied from 2.6 to 15.5 (mean  $\pm$  s.d.,  $7.7 \pm 4.2$ , includes both the primaries and the metastases) and the  $K_i$  values from 0.008 to 0.074  $\text{min}^{-1}$  ( $0.036 \pm 0.023$ ) (Table 2). The SUVs in  $^{11}\text{C}$ -methionine studies varied from 3.2 to 12.4 ( $7.7 \pm 2.5$ ) and  $K_i$  values from 0.063 to 0.311  $\text{min}^{-1}$  ( $0.128 \pm 0.068$ ). The influx constants were always higher in  $^{11}\text{C}$ -methionine studies than in FDG studies. The greatest difference in the SUVs was found in the recurrent acinar cell cancer of Patient 6 (the time interval, 15 days). In Patient 12, the time interval between PET studies was 23 days. The mean difference between SUVs in this case (primary tumor and neck metastases) was 3.2, which was not significantly

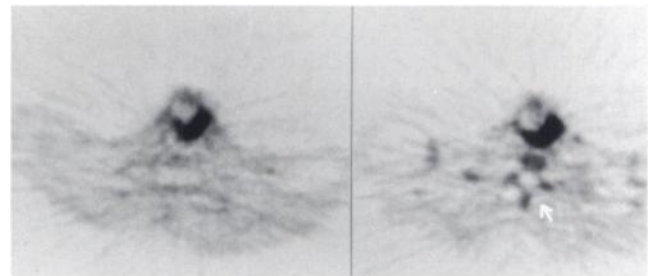


**FIGURE 4.** The hypopharyngeal cancer of Patient 13 is as clearly visualized in the FDG study (left) as in the  $^{11}\text{C}$ -methionine study (right). Carbon-11-methionine accumulates moderately in the vertebra (white arrow), but the image analysis is not impaired.

**TABLE 2**  
Uptake of FDG and <sup>11</sup>C-methionine in Head and Neck Cancer

Patient	Histological grade	SUV		K <sub>1</sub> value min <sup>-1</sup>	
		FDG	Methionine	FDG	Methionine
1	II	3.4	3.7	0.012	—
2	II	8.7	9.0	0.056	0.215
neck		2.6	3.2	0.016	0.079
3	II	10.3	7.5	0.047	0.176
4	III	13.3	8.4	0.062	0.115
neck dx		3.2	6.0	0.013	0.082
neck sin		4.9	5.8	0.019	0.083
5	III	4.4	6.7	0.008	0.077
6	I	2.7	8.1	0.009	0.107
7 neck dx	III	—	4.1	—	0.063
neck sin		4.9	—	0.037	—
8	I	11.8	9.6	0.053	0.176
9	I	7.0	6.2	0.032	0.079
10	I	6.3	6.7	0.023	0.083
neck		3.6	7.2	0.013	0.079
11	II	5.0	8.8	0.018	0.126
12	III	15.5	12.4	0.074	—
neck dx†		12.1	9.5	0.054	—
neck sin		13.3	9.5	0.064	—
13	I	12.9	11.7	0.074	0.311
neck		NFV†	NFV†		
14	II	8.9	9.8	0.043	0.144
Mean		7.7	7.7	0.036	0.128

\*The highest uptake rates in the neck metastases are presented in the table.

†Not in field of view. Neck dx and neck sin are lymph node metastases on the right and on the left side of the neck, respectively.

greater than the mean value of 2.1 (s.d. 1.8) found in the rest of the patients.

A good correlation was found between SUVs ( $r = 0.79$ ,  $p < 0.0001$ ) and K<sub>1</sub> values ( $r = 0.82$ ,  $p < 0.001$ ) between the two tracers (Figs. 5 and 6). No correlation was found between the uptake rate of FDG or <sup>11</sup>C-methionine and the histological grade of cancer (Figs. 7A and B).

## DISCUSSION

Both FDG and <sup>11</sup>C-methionine are useful for metabolic evaluation of head and neck cancer with PET. Only two of the 21 malignant lesions studied were not visible with both tracers. The bilateral neck metastases of Patient 7 were located close to the submandibular glands and the tongue which might have accumulated relatively higher tracer concentrations than the metastases. The other tumors were clearly visible in PET images with both tracers. Hence, there seems to be minimal difference in the tracers' capability to detect head and neck cancer.

The high uptake of FDG in the brain usually does not disturb the PET analysis of head and neck cancer because of the good distinction between the cerebral and intracerebral areas. However, tumor FDG uptake may diminish if the blood glucose concentration is elevated (24–26). In addition, visualization of tumors in PET-FDG images may be impaired because of high FDG uptake in the tongue and the neck muscles (25). This effect may be mediated through hyperglycemia-induced increase in plasma insulin

concentration (27). Hence, PET-FDG studies may be unreliable in diabetic patients. In the fasting state, low FDG uptake in muscles enhances the tumor-to-normal tissue contrast, making tumor delineation generally easy. Nevertheless, malignant schwannoma of the neck (Patient 5) accumulated FDG poorly, even though the patient had fasted.

FDG and <sup>11</sup>C-methionine have different sites of physiological uptake that can cause different tumor-to-background contrast in the PET images. FDG may accumulate

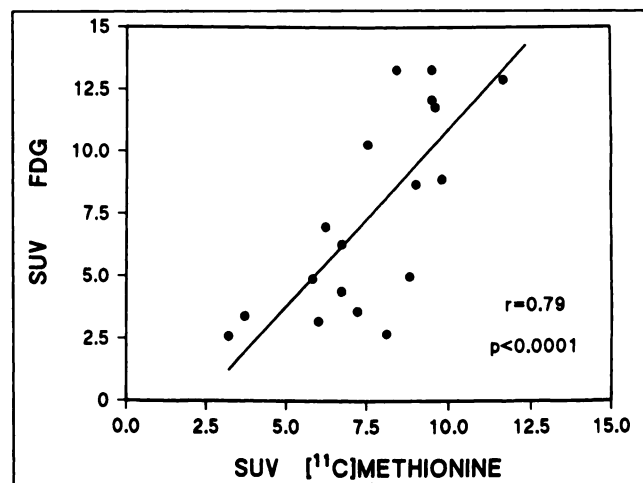


**FIGURE 5.** Correlation between uptake of <sup>11</sup>C-methionine and FDG measured as SUV ( $r = 0.79$ ,  $p < 0.0001$ ).

in lymphoid tissues like the Waldeyer's ring, in the floor of the mouth, and, to a minor degree, in the parotid and submandibular glands and the mucosal tissues. Jabour et al. (28) demonstrated that the sublingual gland had the highest metabolic activity, while FDG activity in bone and striated muscle was negligible. In contrast,  $^{11}\text{C}$ -methionine may accumulate markedly in the lacrimal glands, the salivary glands, and especially in bone marrow (15). Thus, the facial bones that are photopenic areas in FDG studies can often be clearly visible in  $^{11}\text{C}$ -methionine studies. The high tracer uptake in normal tissues may impair analysis of PET images, especially if tumor uptake is low (e.g., Patient 10) or if the tumor is located close to sites of physiological uptake (Patients 6 and 4, Figs. 1 and 2). On the other hand, landmarks like the salivary glands may make it easier to localize the tumor in the PET image.

Both tracers may accumulate in inflammatory processes, which may impair their role in tumor detection and delineation. High FDG uptake in abdominal abscesses has been reported by Tahara et al. (29). Kubota et al. discovered  $^{11}\text{C}$ -methionine uptake in lung granuloma, aspergilloma and abscess (30) and FDG uptake in lung granuloma. Leskinen-Kallio et al. found that  $^{11}\text{C}$ -methionine accumulates slightly in a breast abscess (14).

Only a few studies have compared FDG and  $^{11}\text{C}$ -methionine as oncologic PET tracers. Kubota et al. found that FDG and  $^{11}\text{C}$ -methionine had no significant differences in sensitivity and specificity for the differential diagnosis of lung cancer (30). Leskinen-Kallio et al. (5) found that FDG seemed to correlate better with malignancy grading of non-Hodgkin's lymphoma, but failed to detect some of the low grade lymphomas. Similarly,  $^{11}\text{C}$ -methionine may detect and delineate supratentorial tumors better than  $^{11}\text{C}$ -D-glucose (12). In contrast, pancreatic cancer visualized clearly with FDG while PET imaging with  $^{11}\text{C}$ -methionine could not reliably distinguish pancreatic cancer from a pancreatic cyst or chronic pancreatitis (31).

Surprisingly, the average SUVs of FDG and  $^{11}\text{C}$ -methi-

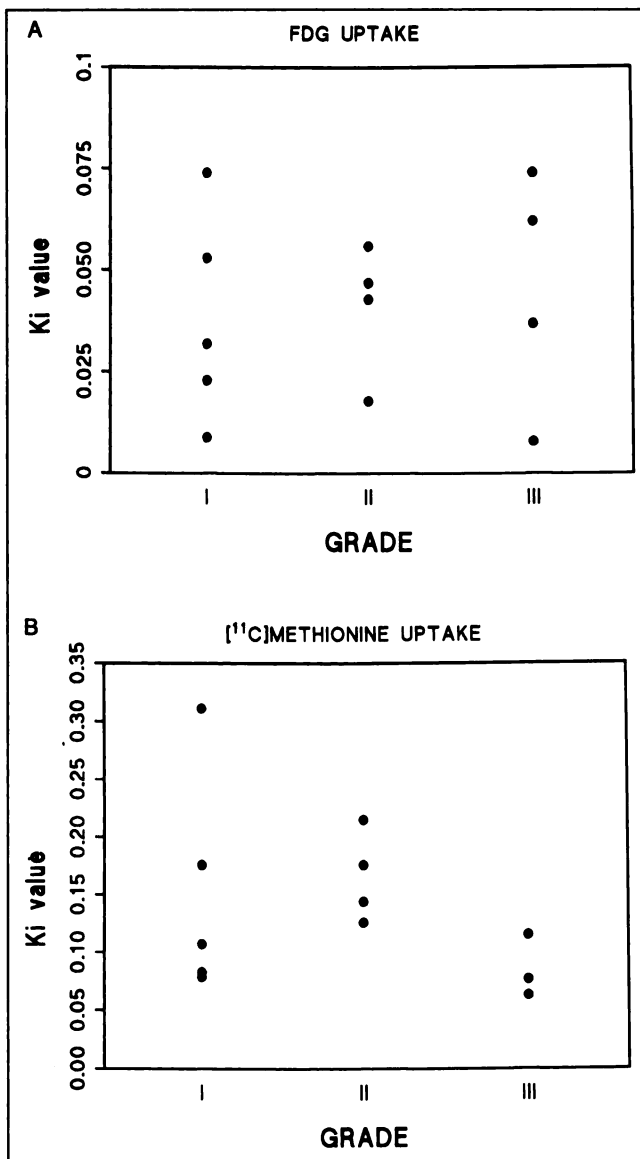


FIGURE 7. (A) Uptake rate of FDG (A) and (B)  $^{11}\text{C}$ -methionine measured as  $K_i$  values as compared with histological grade in head and neck cancer.

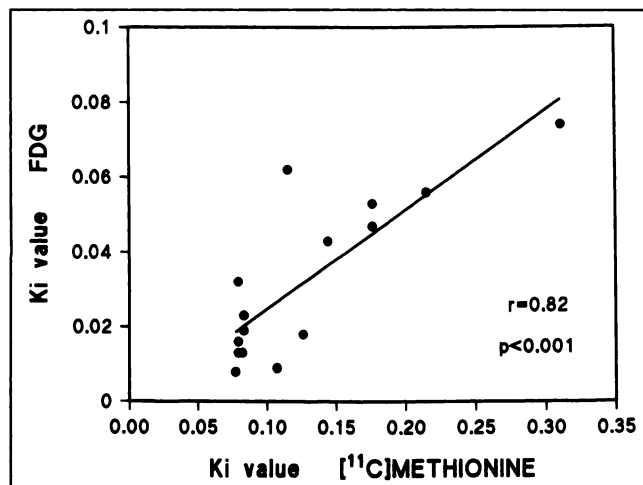


FIGURE 6. Correlation between uptake rates ( $K_i$  values) in  $^{11}\text{C}$ -methionine and FDG studies ( $r = 0.82$ ,  $p < 0.001$ ).

one in the present study were almost identical. Although the  $K_i$  values in  $^{11}\text{C}$ -methionine studies were significantly higher than the  $K_i$  values in FDG studies, the metabolites of  $^{11}\text{C}$ -methionine can deteriorate the contrast between the tumor and blood.

Transport systems of nutrients, such as sugars and amino acids, frequently function at a higher rate in cancer cells and the accelerated transport is likely to be related to the increased proliferation rate of the tumor (32). The good correlation of the uptake rates found in this study may suggest that the uptake rates of glucose and amino acids are equally accelerated in tumor cells. Whether the uptake of glucose and amino acids is associated with the proliferation rate remains to be evaluated in larger series (5,9-10,14).

In conclusion, both FDG and  $^{11}\text{C}$ -methionine are very useful PET tracers in head and neck cancer, and the uptake

rates of the two tracers seem to be closely related in the fasting state. However, both tracers have limitations that should be considered when choosing either tracer for an oncologic PET study.

## ACKNOWLEDGMENTS

We thank professors Eeva Nordman and Uno Wegelius for their support and the personnel of the Cyclotron/PET Center for their cooperation. The Emil Aaltonen Foundation and the Finnish Cancer Society provided financial support for the study.

## REFERENCES

1. Strauss LG, Conti PS. The applications of PET in clinical oncology. *J Nucl Med* 1991;32:623-648.
2. Gallagher BM, Fowler JS, Gutterson NI, MacGregor RR, Chung-Nan W, Wolf AP. Metabolic trapping as a principle of radiopharmaceutical design: some factors responsible for the biodistribution of [<sup>18</sup>F] 2-deoxy-2-fluoro-D-glucose. *J Nucl Med* 1978;19:1154-1161.
3. DiChiro G, DeLaPaz RL, Brooks RA, et al. Glucose utilization of cerebral gliomas measured by [<sup>18</sup>F]fluorodeoxyglucose and positron emission tomography. *Neurology* 1982;32:1323-1329.
4. DiChiro G. Positron emission tomography using [<sup>18</sup>F]fluorodeoxyglucose in brain tumors. A powerful diagnostic and prognostic tool. *Invest Radiol* 1986;22:360-371.
5. Leskinen-Kallio S, Ruotsalainen U, Någren K, Teräs M, Joensuu H. Uptake of carbon-11-methionine and fluorodeoxyglucose in non-Hodgkin's lymphoma: a PET study. *J Nucl Med* 1991;32:1211-1218.
6. Kern KA, Brunetti A, Norton JA, et al. Metabolic imaging of human extremity musculoskeletal tumors by PET. *J Nucl Med* 1988;29:181-186.
7. Griffith LK, Dehdashti F, McGuire AH, et al. PET evaluation of soft-tissue masses with fluorine-2-deoxy-D-glucose. *Radiology* 1992;182:185-194.
8. Okazumi S, Isono K, Enomoto K, et al. Evaluation of liver tumors using fluorine-18-fluorodeoxyglucose PET: characterization of tumor and assessment of effect of treatment. *J Nucl Med* 1992;33:333-339.
9. Minn H, Joensuu H, Ahonen A, and Klemi P. Fluorodeoxyglucose imaging: a method to assess the proliferative activity of human cancer in vivo. Comparison with DNA flow cytometry in head and neck tumors. *Cancer* 1988;61:1776-1781.
10. Haberkorn U, Strauss LG, Reisser Ch, et al. Glucose uptake, perfusion, and cell proliferation in head and neck tumors: relation of positron emission tomography to flow cytometry. *J Nucl Med* 1991;32:1548-1555.
11. Hoffman RM. Unbalanced transmethylation and the perturbation of the differentiated state leading to cancer. *BioEssays* 1990;12:163-166.
12. Ericson K, Lilja A, Bergström M, et al. Positron emission tomography with ([<sup>11</sup>C]methyl)-l-methionine, [<sup>11</sup>C]d-glucose, and [<sup>68</sup>Ga]EDTA in supratentorial tumors. *J Comput Assist Tomogr* 1985;9:683-689.
13. Kubota K, Matsukawa T, Ito M, et al. Lung tumor imaging by positron emission tomography using C-11 L-methionine. *J Nucl Med* 1985;26:37-42.
14. Leskinen-Kallio S, Någren K, Lehtikoinen P, Ruotsalainen U, Joensuu H. Uptake of <sup>11</sup>C-methionine in breast cancer studied by PET. An association with the size of S-phase fraction. *Br J Cancer* 1991;64:1121-1124.
15. Leskinen-Kallio S, Någren K, Lehtikoinen P, Ruotsalainen U, Teräs M, Joensuu H. Carbon-11-methionine and PET is an effective method to image head and neck cancer. *J Nucl Med* 1992;33:691-695.
16. Derlon J-M, Bourdet C, Bustany P, et al. [<sup>11</sup>C]L-methionine uptake in gliomas. *Neurosurgery* 1989;25:720-728.
17. Fujiwara T, Matsukawa T, Kubota K, et al. Relationship between histologic type of primary lung cancer and carbon-11-L-methionine uptake with positron emission tomography. *J Nucl Med* 1989;30:33-37.
18. Olefsky JM. Obesity. In: Wilson JD, Braunwald E, Isselbacher KJ, Petersdorf RG, Martin JB, Fauci AS, Root RK, eds. *Harrison's principles of internal medicine (Vol. 1)*. 12th ed. New York: McGraw-Hill; 1991:411.
19. UICC. International Union Against Cancer. *TNM classification of malignant tumours*. 4th ed. Geneva 1987.
20. Hamacher K, Coenen HH, Stöcklin G. Efficient stereospecific synthesis of no-carrier-added 2-[<sup>18</sup>F]-fluoro-2-deoxy-D-glucose using aminopolyether supported nucleophilic substitution. *J Nucl Med* 1986;27:235-238.
21. Bergman J, Haaparanta M, Solin O. Computer controlled synthesis of 2-[<sup>18</sup>F]fluoro-2-deoxy-D-glucose (FDG). In: Heselius S-J, ed. *The Åbo Akademi accelerator laboratory triennial report 1990-1992*.
22. Långström B, Antoni G, Gullberg P, et al. Synthesis of L- and D-[methyl-<sup>11</sup>C]methionine. *J Nucl Med* 1987;28:1037-1040.
23. Patlak CS, Blasberg RG, Fenstermacher JD. Graphical evaluation of blood-to-brain transfer constants from multiple-time uptake data. *J Cereb Blood Flow Metab* 1983;3:1-7.
24. Wahl RL, Henry CA, Ethier SP. Serum glucose: effects on tumor and normal tissue accumulation of 2-[<sup>18</sup>F]-fluoro-2-deoxy-D-glucose in rodents with mammary carcinoma. *Radiology* 1992;183:643-647.
25. Lindholm P, Minn H, Leskinen-Kallio S, Bergman J, Ruotsalainen U, Joensuu H. Influence of the blood glucose concentration on FDG uptake in cancer—A PET study. *J Nucl Med* 1993;34:1-6.
26. Langen K-J, Braun U, Rota Kops, et al. The influence of plasma glucose levels on fluorine-18-fluorodeoxyglucose uptake in bronchial carcinomas. *J Nucl Med* 1993;34:355-359.
27. Minn H, Leskinen-Kallio S, Lindholm P, et al. [<sup>18</sup>F]Fluorodeoxyglucose uptake in tumors: kinetic versus steady-state methods with reference to plasma insulin. *J Comput Assist Tomogr* 1993;17:115-123.
28. Jabour BA, Choi Y, Hoh CK, et al. Extracranial head and neck: PET imaging with 2-[<sup>18</sup>F]-fluoro-2-deoxy-D-glucose and MR imaging correlation. *Radiology* 1993;186:27-35.
29. Tahara T, Ichiya Y, Kuwabara Y, et al. High [<sup>18</sup>F]-fluorodeoxyglucose uptake in abdominal abscesses: a PET study. *J Comput Assist Tomogr* 1989;13:829-831.
30. Kubota K, Matsukawa T, Fujiwara T, et al. Differential diagnosis of lung tumor with positron emission tomography: a prospective study. *J Nucl Med* 1990;31:1927-1933.
31. Oikawa H, Takahashi H, Yoshioka T, et al. Differential diagnosis of pancreatic diseases using PET. *CYRIC Annual Report* 1991;274-282.
32. Ruddon RW. *Cancer biology, second edition*. New York: Oxford University Press 1987:216-217.